

Vibrational dynamics and thermodynamics, ideal glass transitions and folding transitions, in liquids and biopolymers

C. Austen Angell*, Li-Min Wang*, Stefano Mossa**, Yuanzheng Yue[#], and John R. D. Copley[@].

*Dept. of Chemistry and Biochemistry, Arizona State University, Tempe, AZ 85287

[#]Department of Chemistry, Aalborg University, 9220 Aalborg, Denmark

[@]National Institute of Standards and Technology, Gaithersburg, MD 20899-8562

[‡]Scottsdale Community College, Scottsdale, AZ 85256-2626

**Center for Statistical Mechanics and Complexity

**Universita di Roma "La Sapienza", Piazzale Aldo Moro 2, I-00185, Roma, Italy

Abstract. We use recent studies on hyperquenched glasses, both laboratory and computer simulated, to demonstrate that boson peak vibrations become more intense with increasing fictive temperature, and that this forces a revision of the standard textbook rendering of glass transition thermodynamics. The correct depiction depends on the thermodynamic condition, constant volume or pressure. The absence of a boson peak in glassy water, along with other dynamic and thermodynamic data, is used to argue that water yields the most ordered (near-ideal) glass, due to cooperativity. The similarity of events in this transition, to the folding of proteins into the native form, is emphasized by "funnel" diagrams, in which diversion to fibril states of proteins is seen as the analog of cubic ice formation from deeply supercooled water. A method of studying the energetic details of protein folding, using a special solvent to suppress ice formation and aggregation, is described.

INTRODUCTION

In laboratory studies of glassformers, the natural thermodynamic condition is that of constant pressure, usually that of the atmosphere. By contrast, the "default" condition for theoretical and computer simulation studies, is that of constant volume. This is primarily because of the fact that systems at constant volume provide a simpler target for analysis. For instance, the potential energy landscape, that is so frequently invoked in discussions of complex systems, is only uniquely defined by the potential of interaction of the particles if the volume remains constant [1-3]. If the volume changes, the landscape changes. Also for computer simulations, the calculations are simpler and less time-consuming if the periodic box within which the particles interact, remains constant in volume throughout the calculation. In this paper we first examine some problems in the science of "glasses" that can arise from this cultural distinction.

The data we will use for this purpose, taken from a recent computer simulation of the single component fragile glassformer, orthoterphenyl (OTP) [4,5], will show us that a diagram widely used in the glass science literature to illustrate changes in degrees of freedom on passage through the glass transition, is incorrectly interpreted in most discussions unless the liquid in question has no change in thermal expansion coefficient at T_g (which is not the case in the vast

majority of glassforming substances). The same data will serve to illustrate the behavior of the much discussed "boson" peak in this type of system.

This will provide the motivation for examining the corresponding behavior in laboratory systems, which can only be obtained by employing great variations in the rate at which samples of glass for study are cooled into the glassy state. We will compare the properties of glasses formed by "hyperquenching" (cooling at a rate of 10^6 K/s) [6-9] with the properties of those formed by cooling at the "standard rate" of 20K/min. This will allow us to identify the boson peak intensity with the level of disorder in the system, introduced by change of "fictive" temperature. The fictive temperature of a constant pressure system is usually taken as the temperature at which the system departed from equilibrium during cooling. This is best chosen as the temperature at which the property which changes through the glass transition (e.g heat capacity) is half way between its ergodic and final glassy values. This choice is made so that, for systems cooled and heated at the same rate, the fictive temperature is the same as the common "onset heating" glass temperature [10,11].

In landscape terms (Fig. 1), the change of fictive temperature from standard glass to hyperquenched glass values is that associated with moving the system point from a low level on its energy landscape to a higher level on a *different* energy landscape, namely that characteristic of the system at the volume

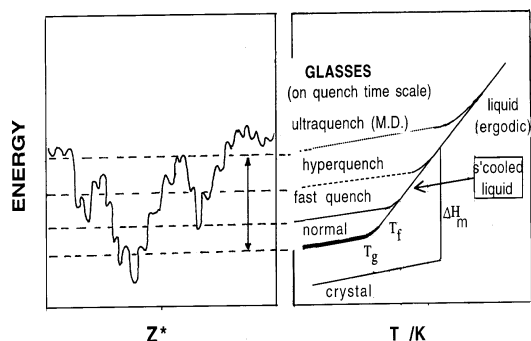


FIGURE 1. Depiction of the relation between the energy of glasses and the rate of quenching. LHS shows the trapped system energy in relation to its energy landscape, represented in the common (but highly over-simplified) two dimensional form appropriate to constant volume systems.

that it had when arrested during the hyperquench. For economy, we show only a single landscape in Fig. 1, which must therefore be thought of as representing a system with a negligible expansion coefficient. Once we have established the height of the boson peak as a measure of disorder in the system, we will look for glassy systems of very low disorder, judged by magnitude of the boson peak obtained from low energy neutron scattering studies. We find such a case in water vitrified by pressure amorphization, followed by relaxation to the low density amorphous (LDA) state [12]. This glassy state of water is similar to, though not identical with [13], the state of water produced by (a) hyperquenching and annealing tiny droplets of water, and (b) by vapor deposition of water onto a cryosurface, and then "sintering" the deposit. Following additional physical evidence that this state of water is a glassy state of unusually low levels of disorder [14-16], we confirm the physical evidence by reference to independent measurements of the entropy of LDA which establish it to be of extraordinarily small "excess" entropy.

The process of forming such a nearly ideal glass [14], can be represented, in energy landscape terms, by descent within an energy "funnel", very similar to that invoked for the description of the mesoscopic complex systems represented by proteins [17]. (Proteins of the small globular type are frequently found to fit the description "two-state folder" [18]). It is even more like the "folding funnel" of the typical two-state protein that must be invoked subsequent to the discovery by Dobson and co-workers [19] that there is generally available a further low energy state for proteins. This is the "fibril" state which involves an organized aggregate of identically folded molecules which may not be in the lowest energy state for the individual molecule, but in which the average free energy is lower than that of same number of optimally folded protein molecules in solution. The "fibril state" [19] is the equivalent, for proteins, of the crystalline state of water molecules.

Excluding the fibril state, we will then show how our exploitation of the cooling rate variable (quenching strategies) can be applied to obtain extra information of a useful type on the energetics of protein folding, using the case of lysozyme.

THE BOSON PEAK, AND THE GLASS TRANSITIONS AT CONSTANT PRESSURE VS. CONSTANT VOLUME

In Fig. 2 we show the results of some computer simulation studies of systems that have a common pressure, 200 MPa. The particular property represented in Fig. 2 is the density of vibrational states $G(\omega)$ for the inherent structure at each of three different temperatures. For inherent structures the temperature corresponds to the fictive temperature. Since the inherent structure for a given temperature is not unique but rather has a statistical probability over a narrow band of energies, the three different $G(\omega)$ values should not be thought of as unique to each temperature, but rather as representative. We note that $G(\omega)$ for the glass of highest fictive temperature is considerably richer in low frequency modes than are the other two and the difference is systematic with temperature. The boson peak, that has been identified from light scattering studies [20-22] is related to the excess density of states as $G(\omega) - \omega^{-4}$ [23]. We show the boson peak implications of the Fig. 2 data in Fig. 3 where the boson peak is seen to gain in intensity and decrease in peak frequency with increasing fictive temperature.

While experimental studies of glasses of different fictive temperature have been made [24], the range of fictive temperatures has been small, and the effects observed also small. We recently showed that much larger effects could be obtained by studying the DOS of hyperquenched glasses. Results are shown in Fig.

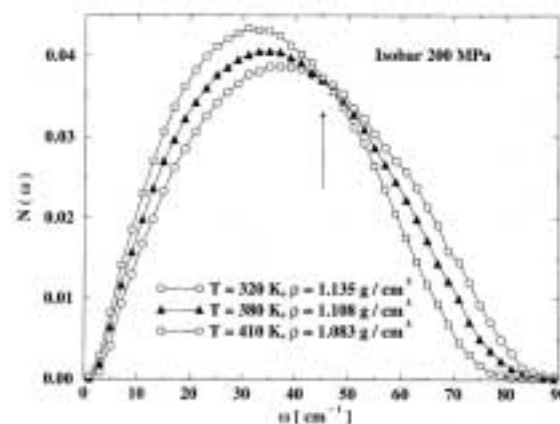


FIGURE 2. The vibrational density of states VDOS for orthoterphenyl OTP at 2000 mPa, in the Lewis-Wahnström model, showing the manner in which, at constant pressure, the increase of temperature causes an increase in the density of states at low frequency at the expense of modes of high frequency (from ref. 9 by permission).

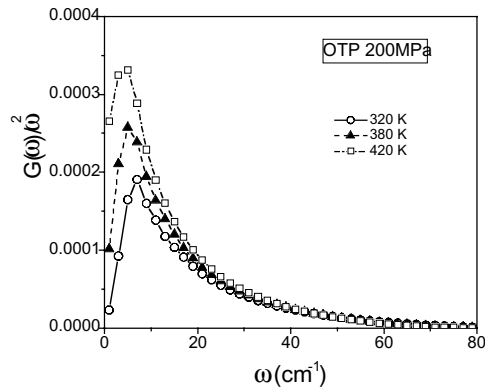


FIGURE 3. Data of Fig. 2 shown in the Boson peak representation ($G(\omega)/\omega^2$). The boson peak is seen to increase in intensity and move to lower frequencies as fictive temperature is increased.

4 for a mineral glass of basalt composition of which hyperquenched samples were readily available [8]. In this case, the DOS changes were also studied for a restricted range of Q vectors, corresponding to the distances 6-11Å in real space. The data, shown in lower part of Fig. 4, imply that the disordering occurs by generation of structures with a specific size. This suggests that a sort of point defect with a narrow distribution of topologies may serve as the elementary excitation in these systems [9].

Even more striking effects in the boson peak behavior have been obtained in recent studies of the fragile CaO-SiO₂ system, which will be published separately [25].

Thermodynamic Consequence of Increased Low Frequency DOS at High Fictive Temperature

In assessing the "configurational" heat capacity of liquids, it has rather generally been the practice to simply extrapolate the glassy state heat capacity to temperatures above T_g , using the behavior of the glass up to T_g , and the crystal above T_g , as a guide [26,27]. In making this construction, it is assumed that the vibrational heat capacity behaves like that of the crystal (fixed structure) regardless of how high the fictive temperature is. This amounts to assuming that the shapes of the basins on the energy landscape (crudely represented on the LHS of Fig. 1) are not changing with height on the landscape. The data of Figs. 2 and 4 show that this is not the case at all, for at least one simulated single component molecular system and one multicomponent ionic system. Since these two systems are almost totally unrelated, it is reasonable to assume that their behavior represents the general case. (However, it would be surprising and provocative if the simple manner in which the vibrational spectrum can be divided up into three

Gaussian components, the central member of which does not change with changing fictive temperature [9], were found to be general).

If the latter is indeed the general case then we need to examine the consequences of the changing DOS quantitatively, to see how greatly the general picture must be modified.

To assess the thermodynamic consequences of the generation of low frequency modes of Fig. 2 at the expense of the high frequency modes with increasing fictive temperature (seen in Fig. 2) we simply apply the harmonic oscillator heat capacity equations to each of the three DOS, to obtain the harmonic vibrational entropy from 0K to the fictive temperature. The harmonic vibrational entropy of each glass (each inherent structure) is shown in Fig. 5. The vibrational entropy of the supercooled liquid at different temperatures can be assessed by joining the values of the vibrational entropy at each fictive temperature together, since the states giving the three DOS of Fig. 2 are the ergodic states at the respective fictive temperatures. It is shown in Fig. 5 as a dashed

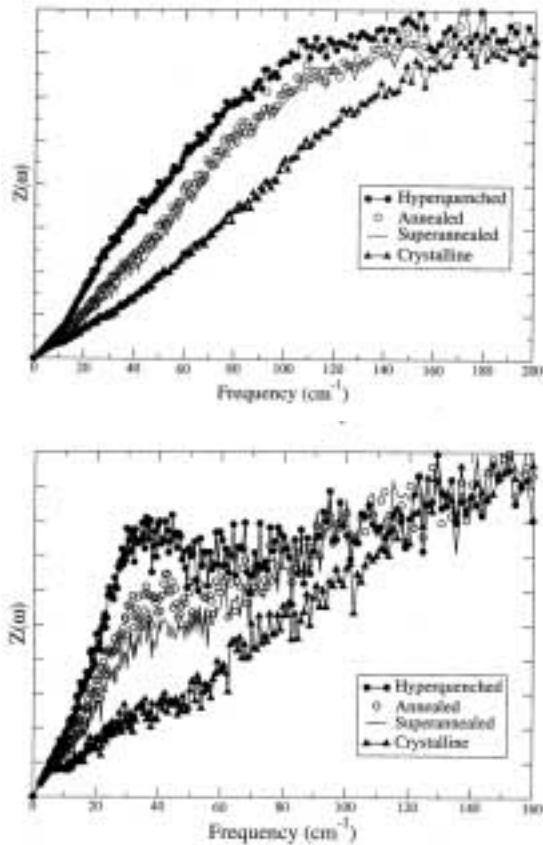


FIGURE 4. Low frequency part of the VDOS for a laboratory system, showing the effect of temperature on the intensity of low frequency modes qualitatively like Fig. 2. Fig. 4, lower part, shows the same data from the same study now restricted in Q values to those corresponding to the distance range $2_\perp/Q$ of 6-11Å, suggesting that some sort of spatially confined defect is involved in the excitations. (From ref. 9, by permission)

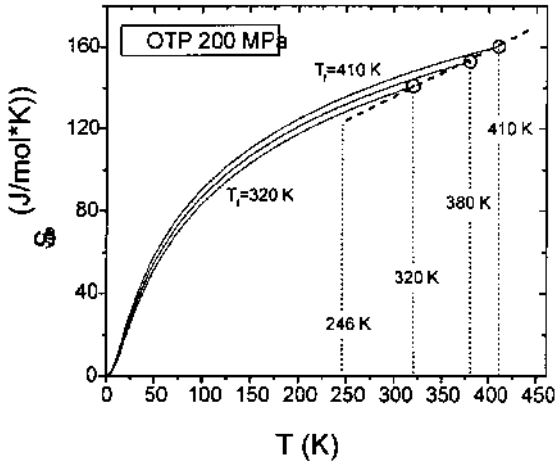


FIGURE 5. Vibrational entropies of the three glasses whose VDOSs are shown in Fig. 2. The lines each stop at the fictive temperature for the glass since at higher temperatures the system would move to a higher energy level of basins and the VDOS will change. The difference in total entropy between glasses, caused by the different populations of low frequency modes is not great. However, the *slope* of the vibrational entropy vs temperature of the equilibrated liquid at constant pressure ($T = T_f$), obtained by joining the end-points of each curve – see dashed line) is very different from that of the single glass. The single glass C_p is similar to that of the crystal, whose structure also remains fixed during heating. In Fig. 5, the ergodic liquid $C_p(\text{vib})$ has been extrapolated to the experimental T_g , 246K.

line. It is clear from the dashed line in Fig. 5, that the rate of *vibrational* entropy increase in the (ergodic) liquid state of this system is very different from any individual fixed structure glass. Since the crystal has fixed structure, the vibrational entropy behavior of the liquid is therefore also very different from that of the crystal which has served as a guide for the vibrational properties of the supercooled liquid in most previous representations of glassy system thermodynamics (represented by Fig. 6a). How different, will be assessed after making the following important point.

The deviation of actual behavior from previously supposed behavior we have just described is only for the *constant pressure* system. When the same analysis is applied to the results obtained at constant volume [4], the opposite situation applies. In the constant volume case, high temperatures favor high frequency modes [4,28], and so the rate of entropy increase above T_g will be *smaller* than for the crystal. When the temperature dependence of the vibrational contribution to the total entropy is extrapolated to the lower fictive temperature of T_g (inaccessible to simulation), we can obtain an idea of what the total excess vibrational entropy (i.e. excess over crystal of fixed structure) should be like relative to the glass value (dashed line in Fig. 5). Indeed, it is very like that sketched in Fig. 4 of Ref. 29.

The continuous change in slope at T_g in Fig. 5 means that there is an almost discontinuous change in

vibrational heat capacity due to the unfreezing of the structure. The change must be as abrupt as the change in total heat capacity registered in a differential scanning calorimetry scan through T_g . However, to the best of our knowledge, this change in vibrational heat capacity has never been rendered in any graphical representation of the heat capacity behavior. It is therefore represented explicitly in Fig. 6 part (b). The corresponding breakdown of the contributions to the total heat capacity that would be measured at constant volume, is shown in Fig 6 part (c).

This analysis warns us that the configurational heat capacity of liquids, which is the total measured heat capacity less the vibrational heat capacity, is much lower than is normally supposed, at least for fragile liquids of the OTP type. Although this effect has been known since Goldstein's analysis in 1972 [30], it has been generally been disregarded as a small effect, which we see here is by no means correct. It will therefore be necessary to take a more careful look at the vibrational heat capacity of glasses as a function of fictive temperature before deciding what the *configurational* entropy of a given liquid actually is. It will considerably change at least two types of analyses of glassy system thermodynamics [27,31] in which the behavior of the vibrational heat capacity was not properly taken into account.

Firstly it will complicate the application of the Adam-Gibbs equation to the analysis of such quantities as the minimum size cooperative group as a function of temperature [27], and will in fact cause the revision of all such numbers *upward*. This will be a welcome change since the numbers obtained from the careful analyses of Yamamuro Matsuo, and coworkers [27] have seemed to be unphysically small. Secondly it will considerably change the estimate of the temperature at which a system will reach the "top of its energy landscape. In earlier assessments it was supposed that the vibrational excess heat capacity would not amount to more than some 10% of the excess C_p , and was neglected. The effect will shift the estimate of the $T_{\text{Tot}} 1.69 T_K$ [31] to $2.5 - 3T_K$, as simulation studies would suggest.

BOSON PEAKS, DISORDER, AND THE NEARLY IDEAL GLASSY STATE OF LDA WATER

In the previous section we showed how the generation of vibrational modes of low frequency during the configurational excitation of glasses, had important thermodynamic consequences, and indeed required us to considerably modify some basic conceptions in glass science (Fig. 6). An important implication of Figure 5 is that, at sufficiently low temperatures, the Boson peak and the contribution of its modes to the entropy of the system will disappear. In Fig. 4 of ref. 29 this was depicted as happening at

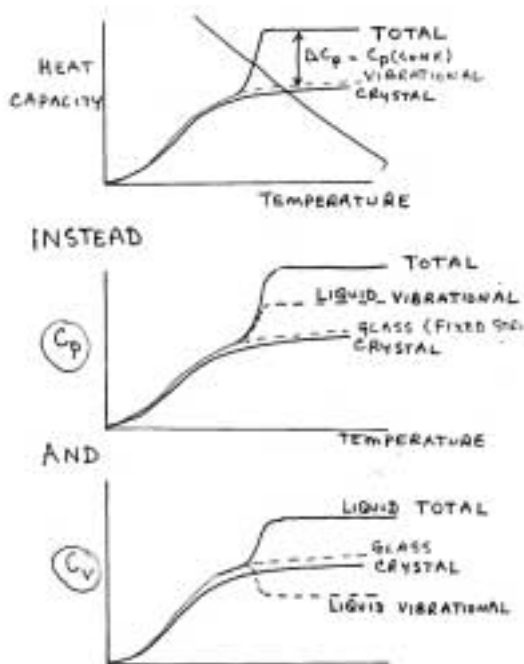


FIGURE 6. (a) Usual representation of the C_p behavior of liquid, crystal and glass states of a substance showing the vibrational component of the heat capacity following the crystal behavior (though somewhat higher).

(b) Correct representation of the same system taking into account the behavior observed for the Lewis-Wahnstrom model, at constant pressure.

(c) Correct representation of the total heat capacity at constant volume, showing the decrease in vibrational heat capacity at T_g required by the oppositely behaving VDOS.

the Kauzmann temperature. Thus the boson peak serves as a spectroscopically accessible measure of structural disorder. We now utilize this aspect of the boson peak as the starting point of an analysis of a particular glass that would appear to be capable of existing in a state of exceptionally low structural disorder, indeed to represent an almost ideal glass state.

The disconcerting aspect of this analysis is that the substance in question, namely, water in its low density amorphous form (LDAW, (or annealed amorphous solid water ASW, or annealed hyperquenched glassy water HQGW), is not normally thought of as a glassforming substance. Our conclusions may well apply to a series of substances that can only be obtained in the glassy state by roundabout routes, but which, when finally vitrified, find themselves in states of very low disorder, as assessed from both dynamic (boson peak etc) and thermodynamic (excess entropy over crystal) criteria.

In a recent review on the subject of Amorphous Water [14], we drew attention to three surprising aspects of the behavior of water in both high and low density vitreous states, HDA and LDA, obtained by the pressure amorphization route. The latter is structurally close to the amorphous states of water

that are obtained by vapor deposition, and by liquid hyperquenching, when each process is followed by some suitable annealing (to remove most of the frozen in disorder) has been carried out. There are minor differences [13] which we will not concern ourselves with here. The advantage of the pressure amorphization route is that large quantities of material can be prepared, with which accurate data are more easily acquired.

The three observations that were notable were, firstly, the absence of a significant excess of low frequency vibrational modes over those of the crystal [15a], i.e. to good approximation the boson peak was missing (from both polyamorphs). Secondly, the LDA sample showed a dispersion relation (obtained from inelastic X-ray scattering) that was almost as well defined as for ice I_c crystals [15b]. Thirdly, the sample of LDA (but not HDA) had a thermal conductivity that increased with decreasing temperature like a crystal [16], meaning the disorder is so small that heat-carrying phonons are not scattered at low temperatures.

Such striking indications of dynamical order are supported by the thermodynamic measurement of order represented by total entropy relative to crystal entropy. The entropy of the LDA phase [32-34] estimated from the measured free energy (from vapor pressure data) and enthalpy data [32] and by other methods [33,34], showed that the excess entropy of LDA over that of ice I_h , is very small. It is only one tenth of the entropy of fusion, compared with 1/3rd for the most fragile liquids in Kauzmann's original comparisons [35]. The analysis of ref. 33 also yielded a value for HDA which, though larger than for LDA, was still much smaller than for other glasses. Thus it seems that, although water is not easily obtained in the vitreous state, once it is obtained in that state it provides an almost ideal, defect-free, example of the glassy state.

This conclusion is consistent with the pattern of behavior of other liquids of varying fragility originally represented by Kauzmann in terms of entropy and temperature variables, scaled by their values at the melting point. We show this diagram, embellished by three other cases of different fragilities [36], in Fig. 7.

We include the vitreous water data in Fig. 7, showing it at the temperature 150 K where it was measured [32]. Just how the connection is to be made between the data acquired above 236 K, where the system is ergodic, and the temperature 150 K where the system is non-ergodic (according to several recent arguments [10,11,14,37,38]), is a matter for discussion. This problem was addressed by Starr et al [39], and their thermodynamically reasoned construction is used in Fig 7. It shows water as the most fragile liquid of all, and the one that, in consequence, reaches the lowest entropy state (relative to the entropy of fusion) before the structure

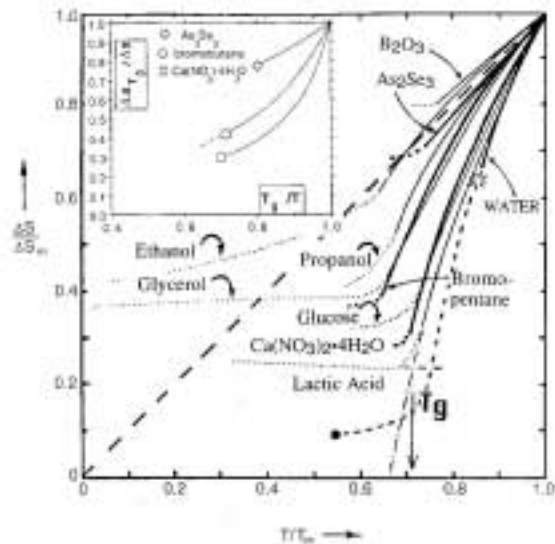


FIGURE 7. Kauzmann diagram, showing excess entropy ΔS vs temperature both scaled by the property at T_m . Added to previous plot [36] is the value for water measured at low temperature, and the connection to high temperature data deduced by Starr et al [39], in order to emphasize the near ideality of glassy water [14]. The starburst on the water plot is the homogeneous nucleation temperature for supercooled water. Here $\Delta S = S_{ex}$. (adapted from Fig. 1 of ref. 36)

becomes fixed by the glass transition. The assignment of relative ideality on the latter basis deserves some discussion. It must be asked if judging the relative ideality of a glass by the fraction of the entropy of fusion that is residual at T_g is appropriate, since it implies something absolute about the entropy of fusion [40]. This is particularly dubious when the system is not glassforming by the usual liquid cooling methods. Substances that are not glassforming by normal cooling methods (usually meaning $T_m/T_g > 1.5$), will have larger entropies of fusion than the same substance would have if it satisfied the $T_m/T_g = 1.5$ rule that applies to most natural glassformers. However, even if water were assigned an entropy of fusion of only half the measured value, it would still have the smallest known relative excess entropy, $S_{ex}(T_g)/\Delta S_{fusion}$ at T_g , so its assignment as thermodynamically the most ideal glass on record would seem secure.

ENERGY FUNNELS AND THE RELATION BETWEEN FORMING THE IDEAL GLASS OF WATER AND THE FOLDING OF PROTEINS

It has become a popular concept to view the progress of a protein from the high temperature unfolded state to the low energy folded state as the progressive descent within an energy "funnel" that guides the system to a final low energy minimum. We believe this is an equally appropriate description

of the way in which the hydrogen bond formation, starting at very high temperatures, guides liquid water into the ideal glass state, even including a cooperative "rush" towards the ground state that sets in at sub-zero temperatures. The cooperative rush is best seen in the heat capacity behavior of supercooled water as deduced for the non-crystallizing case by Starr et al [39], using thermodynamic constraint arguments in combination with available data for glassy and supercooled water. This is shown in Fig. 8 (taken from ref. 39). Fig. 8 is the analog of the heat capacity maximum seen at the changeover from unfolded to folded state that occurs Water is distinguished from the usual representation of the folding protein energy funnel [17] by the presence of an additional narrow (low entropy) energy well representing the crystalline form, see Fig. 9a, the (nucleated) transition to which is unfortunately highly probable. This distinction has, however, recently been diminished by the discovery that proteins in general have an analog lower energy state that can be reached if the system is held long enough close to but below the folding temperature [19]. At this temperature frequent fold-unfold transitions open

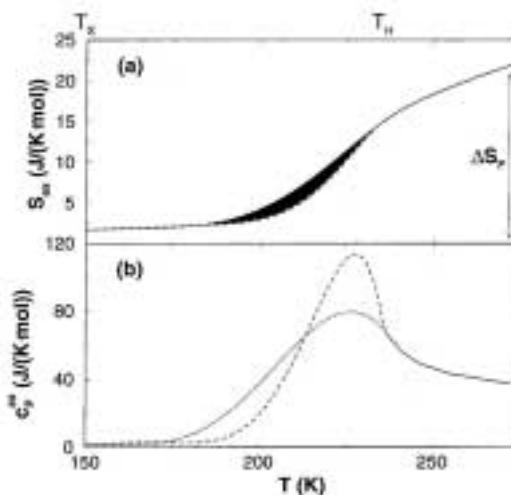


FIGURE 8. The excess entropy (a) and heat capacity (b) of supercooled water in the absence of the renaturation temperature during cooling of a protein. However, for the case of protein folding, the individual molecules fold by fast two-state "on-off" events, and the continuous appearance of the cooling exotherm is due to small system effects. The analogy would be more complete if water were to enter the low temperature, nearly ideal glass, state through a first order liquid-liquid transition such as is known to occur in the topologically similar case of liquid silicon [41,42]. crystallization, deduced by thermodynamic constraint arguments [39] from available data on glassy and supercooled water. The two curves represent the limiting forms permitted by the data uncertainties, excluding the existence of a first order liquid-liquid transition like that in liquid silicon. T_X is near the LDA/ASW crystallization temperature and T_H is the homogeneous nucleation temperature. of supercooled water. (from ref. 39 by permission).

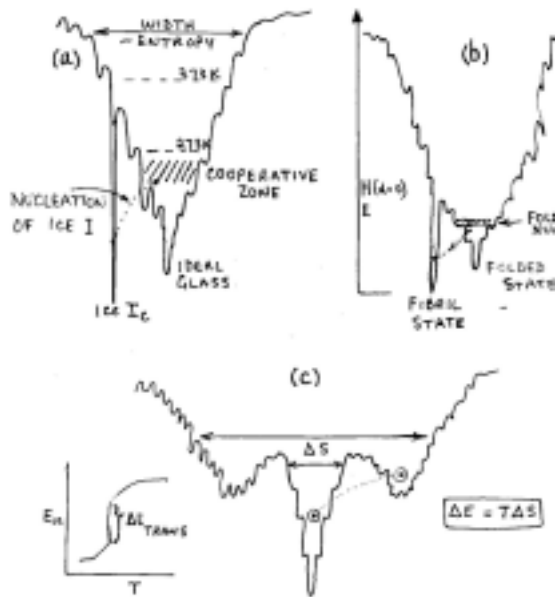


FIGURE 9 (a) Funnel representation of the energy landscape guiding the system water towards the fully hydrogen bonded amorphous ground state. Entropy is represented by the width of the funnel [17]. The narrow and deep well to the left represents the low entropy state of ice Ic, into which the system can transform by a nucleation and growth process.

(b) Funnel representation (Wolynes and co-workers [17]) of the folding of a protein into its low energy (but still conformationally labile) tertiary structure, modified by the addition of a fibril state [19] that is the analog of the crystalline state of normal molecular glassformers. Since the native state is non-periodic, the analogy could be better made with the transformation of liquid silicon in its 4.5 coordinated state, to high temperature

(c) Energy funnel for system with nucleated transitions (two state folding hetero-polymer or liquid-liquid phase transition).

the possibility of aggregation of non-native folded states into the fibril state - which is the analog of ice Ic. In the fibril state, the overall energy per mole of protein molecules is lower, even if the individual molecules are not in their lowest possible energy nucleation event, which requires passage over an energy barrier. The entropy loss implied by the change in basin width is compensated by an energy gain which, at equilibrium, is given by the relation $\Delta E = T\Delta S$, and under metastable conditions is given by the inequality $T\Delta S > \Delta E$. Since we believe the evidence that two-state folding is a nucleated process [43-45], the bottom of the folding funnel would, we suggest, be better represented by the depiction in Fig. 9c. Fig 9c is a symmetrical version of the "two megabasin" representation given originally in ref. 46. configurations. This is because the fibril state has the equivalent of the lattice energy of the usual crystalline state. Fig. 9a,b shows the comparison. In each case the transition from the liquid (molten globule) state to the crystal (fibril) state requires a

Insight into the folding of proteins from experimental analogs of water hyper- quenching studies

To enquire further into the energetics of the protein folding process, we report briefly on some studies, detailed elsewhere [47], in which the folding was suppressed by a fast quenching process equivalent to that which avoids crystallization in the case of water. By use of a novel solvent [48] in which the protein lysozyme can unfold and fold repeatedly without aggregating, and in which no ice forms during cool/heat cycles, we have been able to study the folding of a protein at low temperatures. In cold refolding, as this process may be called, the different energetic steps in the process may be seen. The resolution of the refolding process into distinct stages can be seen by comparison of the heating scan of a quenched sample in which the protein has never left the folded state, with that of a sample quenched from just above the unfolding temperature, 67°C. The whole scan starting from below the glass transition temperature of the solvent (-70 °C) is shown in Fig. 10a. The interesting part, that from the sudden onset of the cold refolding process at about 0°C up to the completion of the folding (which overlaps the restart of the unfolding), is shown in Fig. 10b. Note how closely the second unfolding endotherm overlaps the original unfolding endotherm, proving that essentially no protein was lost to aggregation in the cycle.

There are three aspects of our cold refolding exotherm that are of special interest. The first is that the total energy evolved is the same as that absorbed in the "remelting" at higher temperature, which provides a consistency check for the interpretation of

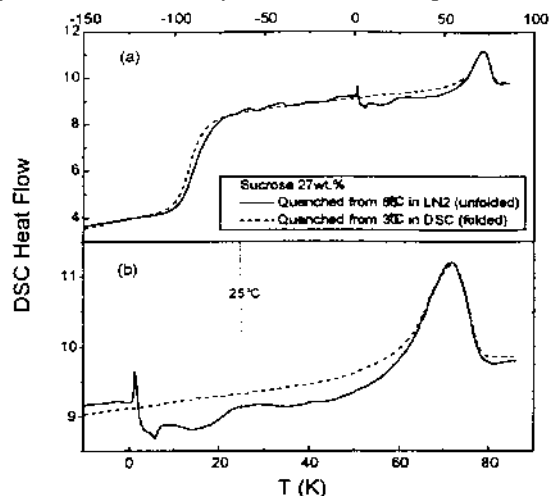


FIGURE 10. Differential scanning calorimetry up scans of LN2-quenched solutions of lysozyme, in the special non-crystallizing non-aggregating solvent developed in this Panel (b) shows a blow-up of this part: the energetic structure of the cold refolding process is revealed. Note the bump at 25°C. The sharp initial exotherm at about 0°C is discussed in text in relation to evidence for a possible nucleation step in the refolding process.

the observed exotherm. We note, with interest and satisfaction, that the enthalpy of work. The dashed plot is for a solution *before* any unfolding has occurred. The solid plot is the same solution quenched from 80K (i.e., after denaturing). This scan shows an exotherm equal in area to the unfolding *endotherm*, suggesting folding was completely suppressed during the quench. unfolding is the same in our solution as it is in normal buffer, notwithstanding the great decrease in water activity that we have affected.

The second aspect of interest is the sudden start to the process at 0°C. At first it was thought that this was an artifact due to ice condensation on the sample pan during transition from the liquid nitrogen quench bath to the DSC sample compartment (since the dry-box in which the process is carried out is simple). Indeed, by subjecting the reference pan to the same quench and mount procedure, it is possible to remove or invert the endothermic spike seen in Fig. 10. However, the sudden start to the refolding exotherm seems to be a robust feature. In this case it requires interpretation. Our tentative interpretation is that this is the temperature at which the system explores its configuration space sufficiently rapidly to nucleate the process by achieving the critical number of native contacts (all of them low energy) to nucleate the final folding into the native state [17b]. This nucleation step is the bottleneck to the process, which can then proceed continuously if not immediately to the final state. Holding the sample at any temperature at 5°C or higher for five minutes is sufficient for the process to go to completion.

Unfortunately we cannot make satisfactory observations of the whole process by isothermal scans at 5°C because of baseline uncertainties.

The way to see the kinetic details of the folding process after its initiation at 0°C is to continuously scan so that the slower parts of the final assembly are encouraged by the higher temperatures, and this constitutes the third item of interest in Fig. 10b. The deceleration (but not arrest) of the folding process seen at 25°C corresponds to the intermediate stage in the lysozyme folding reported by Dobson and coworkers [49-51] using the concentration jump method. In this latter method a solution of protein, denatured by guanidinium chloride, is suddenly diluted to concentrations where the folded state is stable. This alternative method of performing cold refolding studies allows the process to be studied under more natural circumstances than does ours, but does not allow the re-quenching to trap intermediate states with the same efficiency. It would be very good if a microcalorimetry study of the refolding energetics, following concentration jump, could be made for comparison with our isocompositional result.

The conclusion from Fig. 10 is that the folding of lysozyme, rather than being a smooth descent of a

folding funnel as depicted in Fig. 9b, and ref. 17, is much more consistent with Fig. 9c (and Fig. 8 of ref. 43), but with a shoulder structure in the lower energy megabasin. Water vitrification on the other hand, in view of Fig. 8, is probably intermediate between the two, while liquid silicon vitrification during an appropriate hyperquench, is unambiguously Fig. 9c in type, since its first order character has recently been clearly established [42].

It is hoped that further work along these lines, with more detailed thermal studies (including the use of temperature steps such as those used in ref. 45 for the study of nucleation and growth of crystals) might result in an improved understanding of both the thermodynamics of water and the folding of proteins. It is expected that there will be a number of other processes of biological interest in which the use of non-crystallizing solvents such as those used to obtain the Fig. 9 data, will lead to improved understanding of the dynamics and thermodynamics of the processes.

ACKNOWLEDGEMENTS

This work was supported by the NSF-DMR Solid State Chemistry program, under grant no. DMR-0082535. The measurements at NIST utilized facilities supported in part by the National Science Foundation under Agreement No. DMR-0086210.

REFERENCES

1. Goldstein, M., *J. Chem. Phys.* **51**, 3728 (1969).
2. (a) Stillinger, F. H., *Science* **267**, 1935 (1995).
(b) Stillinger, F. H., and Weber, T. A. *Science* **228**, 983 (1984).
3. Stillinger, F. H., and Debenedetti, P. G., *Nature* **410**, 259-267 (2001)
4. Mossa, S., La Nave, E., Stanley, H. E., Donati, C., Sciortino, F., and Tartaglia, P., *Phys. Rev.* **E65**, 041205 [1-8] (2002).
5. La Nave, E., Sciortino, F., Tartaglia, P., De Michele, C., and Mossa, S., *J. Phys. Condens. Matter* **15**, S1085-S1094 Sp. Iss. SI (2003)
6. Chen, H. S., and Inoue, A., Sub-T_g enthalpy relaxation in PdNiSi alloy glasses. *J. Non-Cryst. Sol.* **805**, 61-62 (1984).
7. Huang, J. and Gupta, P., *J. Non-Crystalline Solids*, **151**, 175, (1992).
8. Yue, Y. Z., Christiansen, J. deC., Jensen, and S. L., *Appl. Phys. Lett.* **81**, 2983-2985 (2002).
9. Angell, C. A., Yue, Y. Z., Wang, L.-M., Copley, J. R. D., Borick, S., and Mossa, S., *J. Phys. Cond Mat.* **15**, S1051-S1068 (2003).
10. Velikov, V., Borick, S., and Angell, C. A., *Science*, **294**, 2335-2338 (2001).
11. Angell, C. A., *Chem. Rev.* **102**, 2627-2649 (2002).
12. (a) Mishima, D., Calvert, L. D., and Whalley, E., *Nature* **310**, 393-395. 1984,
(b) Mishima, O. J., *Chem. Phys.*, **100**, 5910 (1994).
13. Johari G. P., Hallbrucker, E., and Mayer, E., *Science* **273**, 90-92 (1996).
14. Angell, C. A., *Annu. Rev. Phys. Chem.* (2004, in press).

- 15 (a) Schober, H., Koza, M., Tölle, A., Fujara, F., Angell, C. A., Bohmer, R., *Physica B.* **241-243**, 897-902 (1998).
 (b) Schober, H., Koza, M. M., Tölle, A., Masciovecchio, C., Sette, F., Ans, A., Fujara, F., *Phys. Rev. Lett.* **85**, 4100 (2000).
16. Andersson, O., Suga, H., *Phys. Rev. B.* **65**:140201(R) (2002).
17. (a) Wolynes, P. G., Onuchic, J. N., and Thirumalai, D., *Science* **267**, 1619-1620 (1995).
 (b) Onuchic, J. N., Luthey Schulten, Z., and Wolynes, P. G., *Annu. Rev. Phys. Chem.* **48**, 545-600 (1997).
18. (a) Privalov, P. I., *Adv. Protein Chem.* **13**, 167 (1979).
 (b) Shakhnovich, E. I., and Finkelstein, A., *Biopolymers* **28**, 1667 (1989).
19. (a) MacPhee, C. E., Dobson, C. M., *J. Am. Chem. Soc.* **122**, 12707-12713, (2000).
 (b) Morozova-Roche, L. A., Zurdo, J., Spencer, A., et al. *J. Struct. Biol.*, **130**, 339, (2000).
20. Duval, E., Boukenter, A., and Achibat, T., *J. Phys. Condensed Matt. Phys.* **2**, 10227 (1990).
21. (a) Malinovsky, V. K., and Sokolov, A. P., *Solid State Communications* **67**, 757-761, (1986).
 (b) Sokolov, A. P., Roessler, E., Kisliuk A., and Quitmann, D., *Phys. Rev. Lett.* **71**, 2062-2065, (1993).
22. Wischnewski, U. Buchenau, A. J. Dianoux, W. A. Kamitakahara and J. L. Zarestky, *Phys. Rev. B* **57**, 2663-2666 (1998).
23. Engberg, D., Wischnewski, A., Buchenau, U., Borjesson, L., Dianoux, A. J., Sokolov, A. P., and Torell, L. M., *Phys. Rev. B* **58** 14 (1998).
24. Suck, J.-B., in *Dynamics of Disordered Materials*, ed. D. Richter, A. J. Dianoux, W. Petry, and J. Teixeira: Springer, Berlin, 1989, p. 182. A related observation is that of Sokolov that the quasi-elastic scattering of an annealed glass is less than that of a quenched glass of the same material at the same temperature.
25. Schober, H., Yue, J., et al, new CaO-SiO₂ results (to be published).
26. Ediger, M. D., Angell, C. A., and Nagel, S. R., *J. Phys. Chem.* **100**, 13200, (1996).
27. a) Takahara, S., Yamamuro, O., and Matsuo, T., *J. Phys. Chem.* **99**, 9589, (1995).
 b) Yamamuro, O, Tsukushi, I, Lindqvist, A, Takahara S, Ishikawa M, Matsuo T *J. Phys. Chem. B*, **102**, 1605, (1998).
28. Sastry, S., *Nature*, **409**, 164. (2001).
29. Martinez, L.-M., and Angell, C. A., *Nature* **410**, 663-667 (2001).
30. Goldstein, M., *J. Chem. Phys.* **64**, 4767 (1976).
31. C. A. Angell, in "Complex Behavior of Glassy Systems" Ed. M. Rubi, Springer, 1997, p. 1.
32. Speedy, R. J., Debenedetti, P. G., Smith, R. S., Huang, C., and Kay, B. D., *J. Chem Phys.*, **105**(1), 240 (1996).
33. Whalley, E., Klug D. D., and Handa, Y.P., *Nature*, **342**, 89 (1989).
34. Kouchi, A., *Nature*, **330**, 550 (1987).
35. Kauzmann, W., *Chem. Rev.*, **43**, 218 (1948).
36. Ito K., Moynihan C. T., and Angell, C. A. *Nature* **398**, 492 (1999).
37. Yue, Y.-Z., and Angell, C. A., *Nature* 2003, (in press).
38. Minoguchi, A., Richert, R., and Angell, C. A., (to be published).
39. Starr, F. W., Angell, C. A., and Stanley, H. E., *Physica, A* **3223**, 51-66 (2003).
40. More appropriate would be the residual entropy per rearrangeable sub-unit of the substance under consideration, but unfortunately there is no definitive method of assigning the number of such sub-units, and simple rigid molecules are in general not glass-forming.
41. Angell, C. A., Borick S., and Grabow, M., *J. Non-Cryst. Solids*, **205-207**, 463-471 (1996).
42. (a) Sastry, S., and Angell, C. A. *Nature Materials*, **2**, 739-743 (2003).
 (b) Angell, C. A., *Physica D* **107**, 122-142 (1997).
43. Shakhnovich, E., Abkevich, V., and Pitsyn, O., *Nature* **379**, 96-98, (1996).
44. Dokholyan, N. V., Buldyrev, S. V., Stanley, H. E., and Shakhnovich, E. I., *Folding and Design* **3**, 577-587 (1998).
45. Dokholyan, N. V., Buldyrev, S. V., Stanley, H. E., and Shakhnovich, E. I., *J. Mol. Biol.* **296**, 1183-1188 (2000).
46. Angell, C. A., *Physica D*, **107**, 122-142 (1997).
47. Angell C. A., and Wang, L.-M., *Biophys. Chem.* **105**, 621-637, (2003).
48. The solvent consists of approximately equal parts of water, ionic liquid (ethyl ammonium nitrate) and sugar (sucrose or glucose, but not fructose or trehalose. The latter exclusions are because of the presence, in the two excluded sugars
49. Matagne, A., Jamin, M. Chung, E. W., Robinson, C. V., Radford, S. E., and Dobson, C. M., *J. Mol. Biol.* **297**, 193-210, (2000).
50. Radford, S. E., Dobson, C. M., and Evans, P. A., *Nature* **358**, 302-307, (1992).
51. Pitsyn O. B., Finkelstein A.V., and Dobson C.M., *Mol. Biol.* **33**, 893-896, (1999).